Acoustic Testing of the Tiltrotor Test Rig in the National Full-Scale Aerodynamics Complex 40- by 80-Foot Wind Tunnel

Natasha L. Schatzman
Aerospace Engineer
NASA Ames Research Center
Moffett Field, CA, USA

Carlos Malpica
Aerospace Engineer
NASA Ames Research Center
Moffett Field, CA, USA

ABSTRACT

The Tiltrotor Test Rig (TTR) was tested in the National Full-Scale Aerodynamics Complex (NFAC) 40- by 80-Foot Wind Tunnel from 2017 to 2018. The primary goal of the test was to understand the operational capabilities of the TTR, while also acquiring research data, including acoustic data. Four microphones were placed around the TTR: two on the wind tunnel floor and two on struts. Acoustic measurements of the TTR rotor were acquired to 1) understand the acoustic testing capabilities of the TTR in the NFAC 40- by 80-Foot Wind Tunnel, 2) compare to previous XV-15 rotor acoustic data acquired in the NFAC 80- by 120-Foot Wind Tunnel, and 3) provide data for future validation studies. A data quality study revealed that the NFAC 40- by 80-Foot Wind Tunnel is an adequate acoustic environment to test the TTR rotor. For a given thrust and advance ratio, a shaft angle sweep was performed and acoustic measurements were compared against 1996 and 1999 XV-15 data in the NFAC 80- by 120-Foot Wind Tunnel; differences between the three tests are discussed.

NOTATION

BPF	Blade passage frequency, $\frac{N_b RPM}{60}$ (Hz)
$BVISPL$	Blade Vortex Interaction Sound Pressure Level (dB; reference: 2×10^{-5} Pa), integrated from filtered spectrum SPL
C_T	Rotor thrust coefficient, $\frac{T}{\rho A V_{tip}^2}$
M_{AT}	Advancing tip Mach number, $(1+\mu)M_{tip}$
M_{tip}	Hover tip Mach number
N_b	Number of blades (per rotor)
$OASPL$	Overall sound pressure level (dB; reference: 2×10^{-5} Pa), integrated from unfiltered spectrum SPL
R	Rotor radius (ft)
RPM	Rotor rotational speed, revolutions per minute
SPL	Sound pressure level (dB; reference: 2×10^{-5} Pa)
T	Rotor thrust (lb_f)
V_∞	Tunnel velocity (ft/s)
V_{tip}	Rotor blade rotational speed at tip (ft/s)
x	Uptream coordinate relative to rotor hub at $\alpha_s = 0^\circ$, positive into the wind
y	Vertical coordinate relative to rotor hub at $\alpha_s = 0^\circ$, positive down
z	Lateral coordinate relative to rotor hub at $\alpha_s = 0^\circ$
α_s	Rotor shaft angle (deg), measured normal to tunnel flow
ω	Rotor rotational speed (rad/sec), counter-clockwise
μ	Advance ratio, V_∞/V_{tip}
σ	Rotor solidity, $\frac{N_b c R}{\pi R^2}$

Presented at the Vertical Flight Society 75th Annual Forum & Technology Display, Philadelphia, Pennsylvania, May 13–16, 2019.

INTRODUCTION

The Tiltrotor Test Rig (TTR) provides the National Aeronautics and Space Administration (NASA) and the Department of Defense (DoD) with a new national test capability to conduct technology development, testing and evaluation of new large-scale proprotors for performance, control, loads, and stability in the National Full-Scale Aerodynamics Complex (NFAC). The TTR is unique because it allows for the universal testing of various rotors instead of having specific configurations for each type of rotor (Ref. 1). This is possible because the TTR is able to rotate using the test-section turntable and operate at various angles from airplane mode to helicopter mode, from 0- to 100-deg shaft tilt angles. The TTR is designed to be used in both the NFAC 40- by 80- and 80- by 120-Foot Wind Tunnels, and it was subjected to a comprehensive checkout test program in the NFAC 40- by 80-Foot Wind Tunnel (Refs. 2, 3). Initial testing of a full-scale proprotor on the TTR was completed in March 2018 with acoustics being one of the program elements. Though various flight conditions were tested, this paper will only present data in helicopter mode, particularity for Blade Vortex Interaction (BVI) flight conditions.

Acoustic Test Objectives

The primary acoustic goal of the TTR test was to measure rotor noise at various BVI flight conditions in order to: 1) understand the acoustic testing capabilities of the TTR in the NFAC 40- by 80-Foot Wind Tunnel, 2) compare acoustic data with

previous tiltrotor tests and 3) provide data for future validation studies. Comparisons will be made against acoustic data from the XV-15 taken in the 80- by 120-Foot NFAC wind tunnel from 1996 and 1999 (Refs. 4–6).

TEST HARDWARE

TTR and Rotor Description

The TTR is a horizontal axis rig mounted in the wind tunnel on a three-strut support system that rotates on the test-section turntable. The turntable can either face the rotor into the wind at high speed (up to 273 knots) for airplane mode or fly edgewise at low speed (up to 120 knots) for helicopter mode, or at any angle in between. Figure 1 shows the downstream view of the TTR in the NFAC 40- by 80-Foot Wind Tunnel in helicopter mode. The NFAC 40- by 80-Foot Wind Tunnel test section walls are treated with acoustically absorbent material to reduce reflections and minimize standing waves that can contaminate the noise field. This provides an absorptivity of greater than 90-percent at frequencies above approximately 100 Hz (Ref. 7).

The rotor tested on the TTR was a 3-bladed research rotor derived from the right-wing rotor of the Leonardo (Agusta-Westland) 609 rotor (Ref. 1). The basic parameters of the checkout rotor on the TTR, designated as Bell Model No. 699, are shown in Table 1 alongside the XV-15 parameters for comparison. The blades were manufactured using the same molds as the production rotor, and therefore twist, blade tip and all other geometric blade parameters are identical. The differences between the TTR rotor and the Leonardo (Agusta-Westland) 609 rotor are that the TTR rotor has no deicing and pendulum absorbers, has additional instrumentation, and the pitch horn lugs are inverted. These differences should have no effect on acoustics measurements.

Table 1. TTR Bell Model 699 and XV-15 rotor parameters (Ref. 1).

Parameter	TTR Bell Model 699	XV-15
Radius (ft)	13	12.5
Number of Blades	3	3
Chord at tip (in)	14.83	14.0
Solidity	0.0908	0.089
Hub precone angle (deg)	2.75	1.5
Twist (deg)	47.5	41 (nonlinear)
Airfoils	XN12 (Refs. 8, 9)	NACA 64-series
Blade tip shape	square	square
Rotor RPM, helicopter mode	569	589
Blade planform	linear taper	constant chord

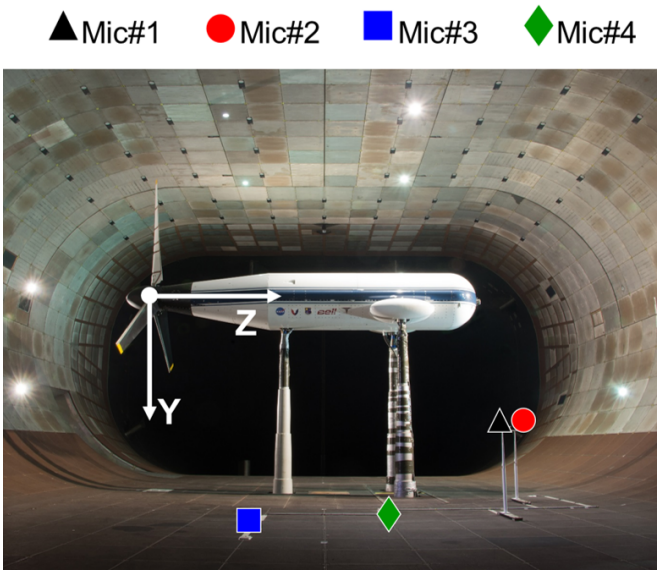

Fig. 1. TTR in helicopter mode with microphone locations in the NFAC 40- by 80-Foot Wind Tunnel test section, view looking downstream

Microphone Placement

Four microphones were placed around the TTR to take acoustic measurements in the NFAC 40- by 80-Foot Wind Tunnel (Tables 2 and 3). Microphones were positioned near the expected peak BVI noise directivity angle, with microphone 3 positioned to match data acquired in both XV-15 tests, while ensuring they did not affect the inflow to the rotor in airplane and conversion modes. Microphones 1 and 2 were mounted on 5.625 ft struts and microphones 3 and 4 were flush-mounted with the test section floor. Table 2 shows the microphone positions with respect to the center of the TTR rotor in helicopter mode, while Table 3 shows the microphone azimuthal and elevation angles. The x-direction is positive in the upstream direction, positive y-direction is downward, and positive z-direction is the cross-flow direction (see Fig. 1).

Tests of the XV-15 rotor were performed in the NFAC 80- by 120-Foot Wind Tunnel in 1996 and 1999 (Refs. 4–6). The acoustic measurements from these two tests will be compared to TTR rotor acoustic measurements. The test in 1996 had six microphones, as shown in Table 2. Microphones 1 through 4 were placed on a traverse under the rotor to capture BVI, while microphones 5 and 6 were placed to match previously acquired flight test data (Ref. 5). The test in 1999 had nine microphones, also shown in Table 2. Microphones 1 through 8 were placed on a traverse under the rotor to capture BVI, while microphone 9 was placed to match previously acquired wind tunnel and flight test data (Ref. 5).

DATA INSTRUMENTATION AND ACQUISITION

All TTR acoustics data were acquired with the NFAC's dynamic data system (DDAS) and a backup system

Table 2. Microphone positions for the TTR test in the NFAC 40- by 80-Foot Wind Tunnel and XV-15 tests in the NFAC 80- by 120-Foot Wind Tunnel, with respect to center of hub in helicopter mode (α_s = 0°).

Wind Tunnel Model	Mic #	X/R	Y/R	Z/R	Distance (R)
NFAC 80- by 120-Foot XV-15 (1996)	1*	0.00	0.58	1.82	1.91
	2*	0.00	0.75	1.82	1.97
	3*	0.00	1.11	1.82	2.13
	4*	0.00	1.46	1.82	2.33
	5	4.87	2.82	2.05	5.99
	6	3.60	-4.20	2.05	5.90
NFAC 80- by 120-Foot XV-15	1*	-0.20	0.35	1.80	1.84
	2*	-0.20	0.54	1.80	1.89
	3*	-0.20	0.74	1.80	1.95
	5*	-0.20	1.12	1.80	2.13
	6*	-0.20	1.31	1.80	2.24
	7*	-0.20	1.51	1.80	2.36
	8*	-0.20	1.70	1.80	2.48
	9	-4.89	2.82	2.05	6.01
NFAC 40- by 80-Foot TTR (2018)	1	1.85	1.07	2.15	3.03
	2	0.92	1.07	2.46	2.84
	3	2.66	1.54	1.12	3.27
	4	2.15	1.54	1.54	3.06

* Denotes microphones on traverse, where X/R is closest distance to the center of the hub.

Table 3. Microphone azimuth and elevation angle for the TTR test in the NFAC 40- by 80-Foot Wind Tunnel and XV-15 tests in the NFAC 80- by 120-Foot Wind Tunnel, with respect to center of hub in helicopter mode (α_s = 0°).

Wind Tunnel Model	Mic #	Azimuth (deg)	Elevation (deg)
NFAC 80- by 120-Foot XV-15 (1996)	1*	90	72
	2*	90	68
	3*	90	59
	4*	90	51
	5	150	20
	6	229	20
NFAC 80- by 120-Foot XV-15 (1999)	1*	120	77
	2*	110	72
	3*	105	67
	4*	102	62
	5*	100	58
	6*	99	54
	7*	98	50
	8*	97	46
	9	150	20
NFAC 40- by 80-Foot TTR (2018)	1	150	45
	2	131	60
	3	150	20
	4	144	30

* Denotes microphones on traverse, where X/R is closest distance to the center of the hub.

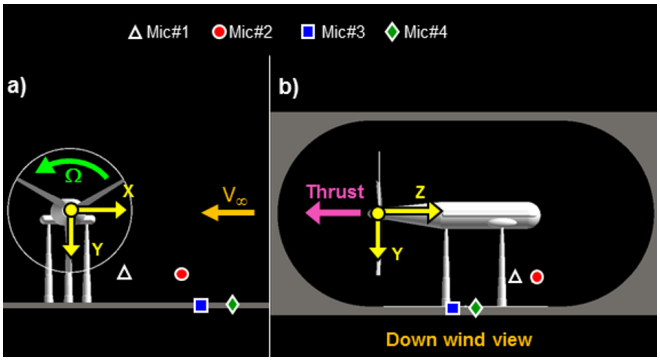

Fig. 2. TTR microphone locations in the NFAC 40- by 80-Foot Wind Tunnel in the a) XY and b) ZY plane.

(DEWETRON TrendCorder). Analog feed from the four microphones was routed from the test section into the acoustics station in the computer room where the microphone power supply (G.R.A.S. 12AG 8-Channel Power Module), the DEWETRON TrendCorder, and the near real-time display were located (see Fig. 3). Microphones 1 and 2 were free-field G.R.A.S. 40AC 1/2" microphones with a G.R.A.S. 26AJ 1/2" preamplifer. Microphones 3 and 4 were precision surface G.R.A.S. 40LS 1/4" CCP microphones used with a G.R.A.S. AG0002 CCP input adapter.

The microphone conditioner served as a power supply for the microphones and provided gain-control as well as a high pass filter for each microphone output signal. Each microphone channel was routed through a 3-pole Butterworth high-pass filter with a –1 dB cut-off at a frequency of 20 Hz. This filter reduced unwanted low-frequency signals, e.g., wind-induced noise on the microphone. The microphone channel gains were set prior to the start of every data point to maximize signal-to-noise ratio. The gain setting values were recorded on the near real-time display computer for each microphone, which was connected to the NFAC DDAS data system. Acoustic time history data (in volts) were subsequently digitized by the DDAS at a sampling rate of 2048 points per revolution for 128 revolutions. A start trigger, 1/rev, and 2048/rev signal were sent from the NFAC to the DEWETRON TrendCorder in order to ensure consistent post processing of the data with the two data systems.

TEST CONDITIONS

The acoustic testing included a sweep of shaft angle (α_s) at an advance ratio (μ) of 0.125, tip Mach number (M_{tip}) of 0.684 and a blade loading coefficient (C_T/σ) of 0.075. Shaft angles included -10, -8, -6, -4, -2, and -1 through 10°. The rotor was trimmed to zero flapping, such that the tip path plane angle of attack is equal to the shaft angle. Acoustic data were analyzed for the shaft angle sweep in order to identify the shaft angle that yielded the peak BVI noise. The shaft angle identified was used in a blade loading coefficient sweep.

A flight condition of C_T/σ = 0.100, μ = 0.125, M_{tip} = 0.684, at α_s = 0° was used to analyze repeatability. Additionally,

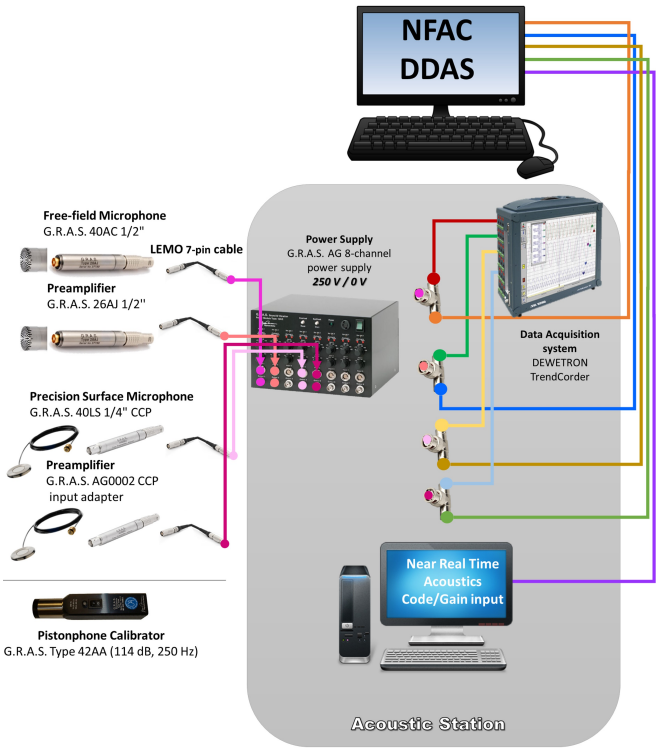

Fig. 3. NFAC 40- by 80-Foot Wind Tunnel acoustics data acquisition station.

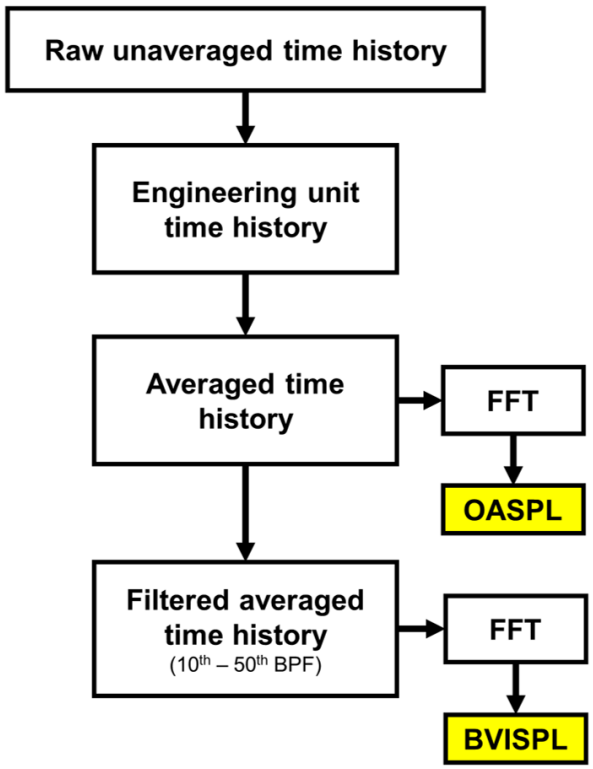

Fig. 4. TTR acoustic data post-processing procedure.

sweeps of advance ratio for $C_T/\sigma = 0.050$ and $C_T/\sigma = 0.100$, at $\alpha_s = -15°$, were performed to show effect of advancing tip Mach number on BVI noise.

DATA POST-PROCESSING

The acoustic data post-processing procedures are shown in Fig. 4. The raw data was first converted from volts to pressure by applying a calibration constant and associated gain input. The converted data was then averaged using all 128 revolutions of data. Filtering and integration were then performed to provide the time histories and acoustic metrics for further analysis.

The two primary acoustics metrics computed are the overall sound pressure level (OASPL) and the blade-vortex interaction sound pressure level (BVISPL). The OASPL is determined by performing a Fast Fourier Transform (FFT) on the averaged acoustic pressure time histories and then integrating the resulting power spectrum. The BVISPL is computed by integrating the spectrum only between the 10th through 50th blade passage frequencies (284.4–1422 Hz). The first blade pass frequency (BPF) for the TTR rotor is 28.45 Hz and 29.45 Hz for the XV-15. A bandpass filter was identified to filter the averaged acoustic pressure time histories prior to the FFT calculation, including all background noise measurements. This frequency band was selected to match the BVISPL metrics for the 1996 and 1999 XV-15 rotor test in the NFAC 80- by 120-Foot Wind Tunnel (Refs. 4–6), and is well within the test section acoustic liner absorption capability for the NFAC 40- by 80-Foot Wind Tunnel (Ref. 7), which is acoustically treated for 100 Hz and above.

Because of the positioning of the TTR, the furthest that microphone 3 could be positioned from the rotor hub was 3.3 rotor radii away, where as microphone 5 from the 1996 test and microphone 9 from the 1999 test in the NFAC 80- by 120-Foot Wind Tunnel were placed at 6 rotor radii away. The difference in propagation distance was accounted for by the inverse-square law (Ref. 10), to adequately compare acoustic metrics between tests.

DATA QUALITY

To investigate the quality of acquired acoustic data in the NFAC 40- by 80-Foot Wind Tunnel for the 2018 TTR test, an analysis was performed on the wind tunnel background noise and TTR acoustic repeatability. For the background noise analysis (blades off), data presented includes a wind tunnel velocity sweep and a shaft angle sweep at 60, 105 and 155 knots. A flight condition performed over multiple runs and days was selected for the repeatability analysis. Consideration was also given to investigate the sensitivity of the BVISPL metric to bandpass filter settings.

There are additional concerns about the quality of the data that arise from the positions of the hardware in the wind tunnel. These many not affect the repeatability, but rather bias the measurements. One concern is that the TTR aerodynamic performance may be affected by the wall proximity. It is noted

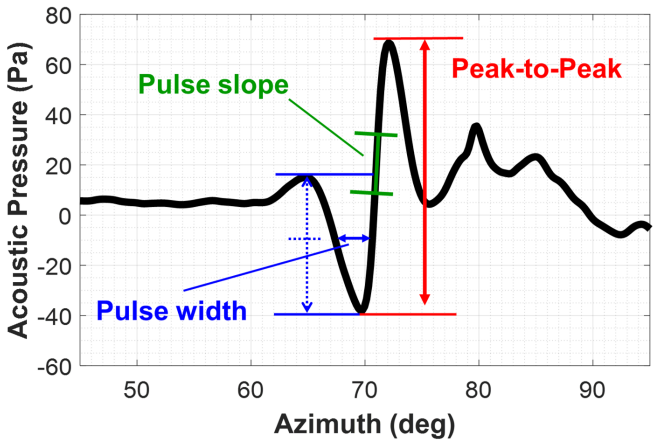

Fig. 5. BVI pulse peak-to-peak, slope, and width identification for one blade passage.

Table 4. Unfiltered and filtered BVI pulse peak-to-peak, slope, and width calculations for microphone 1 (μ = 0.125, M_{tip} = 0.684, C_T/σ = 0.075 and α_s = 0°).

BPF	BVISPL (dB)	Pk-Pk (Pa)	Slope (Pa/deg)	Width (deg)
Unfiltered	117.43	106.7	90.64	3.07
5th-40th	113.61	106.5	62.04	3.19
5th-50th	113.66	107.4	71.23	3.44
10th-50th	113.37	101.2	68.60	2.89
10th-40th	113.31	99.6	58.96	3.10

that in the configuration shown in Fig. 1, the rotor tip is 6.5 feet (y-direction) from the floor/ceiling. The TTR rotor hub center is 19.5 feet from the tunnel wall (negative z-direction from origin). Because microphones 3 and 4 are located on the wind tunnel floor, another concern is they will capture low frequency acoustic (first rotor harmonic is 9.48 Hz) reflections off of the floor. Because of this reason, the acquired acoustic data may be contaminated due to possible reflections and standing waves (Ref. 7). At this time, no corrections have been made to account for reflections, standing wave, or wall proximity.

BVI Bandpass Filtering Considerations

For the BVISPL metric, desired bandpass filter settings are required to preserve the BVI occurrence pulse peak-to-peak, slop and width, while also attenuating potentially contaminating low or high frequency inputs. A graphic defining the pulse peak-to-peak (Pk-Pk), slope, and width is shown in Fig. 5 for one rotor blade passage. The peak-to-peak value is the amplitude of the pulse from the maximum and minimum values. BVI pulse slope is determined at the steepest slope between the maximum and minimum pulse, while the pulse width is the width of the first pulse at 50 percent amplitude.

The effect of different bandpass filter settings for the BVISPL metric are shown in Fig. 6 and Table 4. Though a filter of the 5th through the 50th BPF is probably best, a bandpass filter

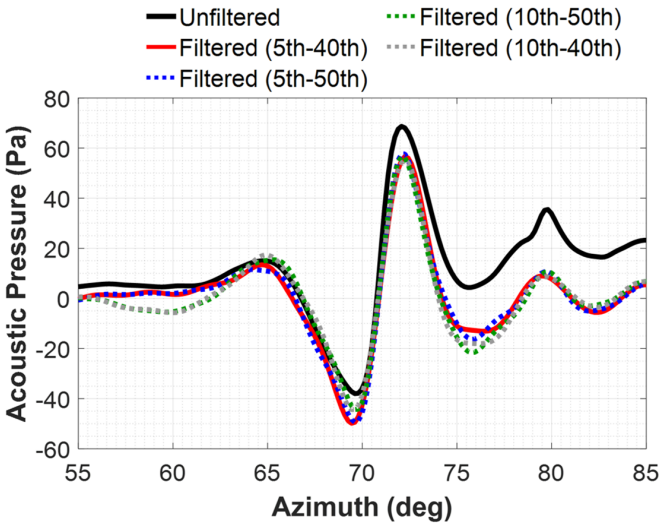

Fig. 6. TTR in the NFAC 40- by 80-Foot Wind Tunnel acoustic time history bandpass filter study for microphone 1 (μ = 0.125, C_T/σ = 0.075 and α_s = 0°).

from 10th to the 50th blade passage was considered adequate and chosen to be consistent with the NFAC 80- by 120-Foot Wind Tunnel test. The calculated BVI pulse peak-to-peak, slope, and width is shown in Table 4 for all filters applied.

Background Noise

Background noise measurements (acoustic tares) were acquired with the rotor hub spinning without blades. The background noise includes the combination of wind noise over the test hardware and microphones, mechanical noise from the hydraulic TTR pump and motor, and tunnel drive noise.

Figure 7 shows the background noise for microphones 1 through 4 for tunnel airspeeds ranging from 0 to 257 knots at α_s = -90° (airplane mode) for OASPL and BVISPL. As expected, both OASPL and BVISPL metrics increase with airspeed, with OASPL always greater than BVISPL.

Background noise for a variation of shaft angle for wind tunnel speed of 60, 105, and 155 knots is shown in Fig. 8 in terms of a) OASPL and b) BVISPL for microphone 1. For OASPL the variation in shaft angle resulted in a delta of 6.05, 8.58, and 6.17 dB for a wind tunnel speed of 60, 105, and 155 knots, respectively. For BVISPL, shaft angle resulted in a delta of 3.90, 4.07, and 2.74 dB for the same airspeeds. The variations in OASPL and BVISPL are likely caused by the wind noise over the TTR at different positions of the TTR.

A comparison of the background noise to a typical rotor-on BVI condition is shown in Fig. 9. Figure 9 a) shows the acoustic time history from microphone 1 at a flight condition of μ = 0.125, M_{tip} = 0.684, C_T/σ = 0.075 and α_s = 0°, and associated background noise (60 knots, α_s = 0°, blades off). Figure 9 b) shows the resultant acoustic frequency spectrum. The OASPL background noise for this condition is 72.4 dB which results in a good signal-to-noise ratio for this flight condition.

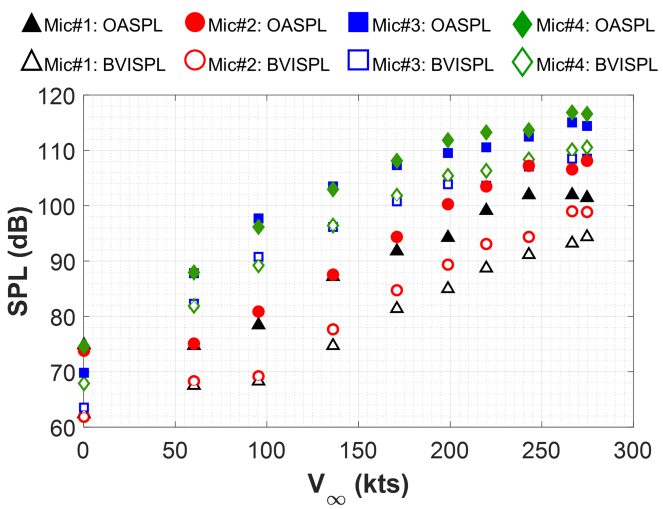

Fig. 7. TTR background noise as a function of airspeed in the NFAC 40- by 80-Foot Wind Tunnel at α_s = -90° (airplane mode) for OASPL and BVISPL.

Repeatability

Data repeatability was evaluated in three ways: a) comparing the rev-to-rev variability for a single data point, b) comparing the blade-to-blade variability for an averaged time history, and c) comparing average time histories for multiple data points.

Figure 10 shows averaged (red) versus the 128 revolutions (gray) of a sample acoustic time history data for microphone 1 for a flight condition of C_T/σ = 0.075, μ = 0.125, M_{tip} = 0.684, and α_s = 0°. The peak-to-peak for each revolution of data was compared to the averaged revolution of data and revealed a maximum of 20% difference, for this data point and microphone.

A blade-to-blade difference can be seen by comparing the peak-to-peak difference of the three pulses. From Fig. 10, the acoustic pressure pulse associated with a blade-vortex interaction with blade one is the first pulse from 70 to 90° azimuth, blade two is the 2nd pulse from 190 to 210° azimuth, and blade 3 is the 3rd pulse from 310 to 330° azimuth. In Fig. 11, the third pulse shows on average a consistently slightly larger peak-to-peak difference compared to pulse one and two. While blades are nominally identical, this could point to slight differences in the tracking of each blade. Acoustically, however, these differences are insignificant.

A flight condition of μ = 0.125, M_{tip} = 0.684, C_T/σ = 0.050 and α_s = 0° was repeated to assess the point-to-point repeatability of the acoustic data, as shown in Fig. 12. Eight points, each from different runs over different days for microphone 1 are shown in Fig. 12. For the repeating flight condition, microphones 1 showed a difference in OASPL of 0.40 dB. Not shown, microphones 2 through 4 measured a comparable difference in OASPL of 0.38, 0.50, and 0.73 dB, respectively. The slight variation in OASPL is due to day-to-day atmospheric conditions and rotor flight condition control.

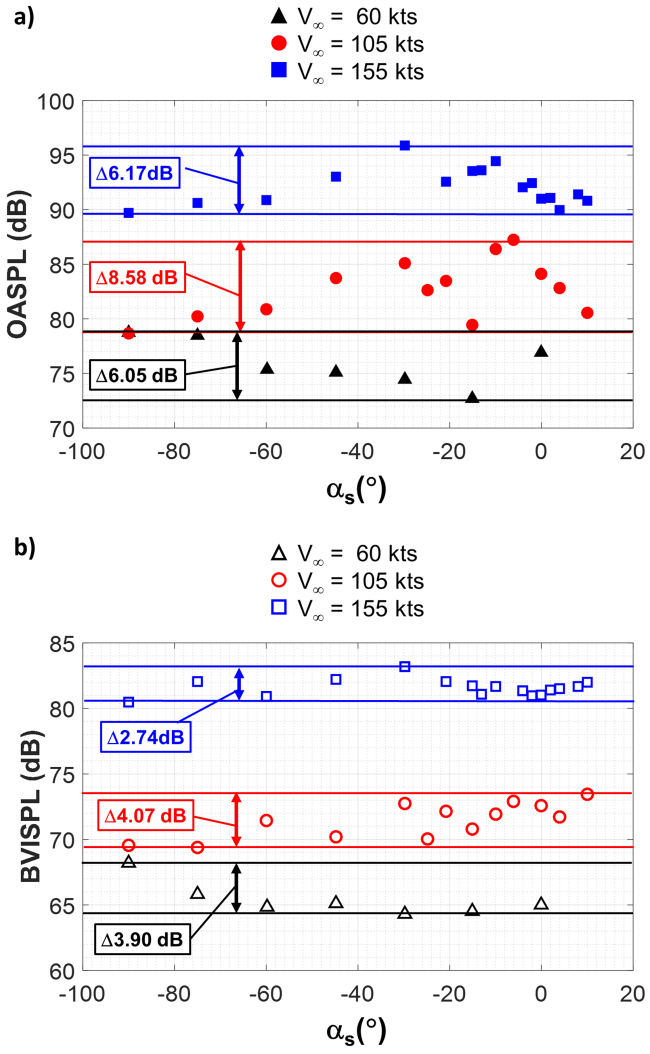

Fig. 8. TTR microphone 1 background noise as a function of α_s in the NFAC 40- by 80-Foot Wind Tunnel at V_∞ = 60, 105, and 155 knots for a) OASPL and b) BVISPL.

RESULTS

Representative time histories and acoustic metrics are presented in this section for various TTR test conditions. Comparisons to acoustic data from the 1996 and 1999 NFAC 80- by 120-Foot Wind Tunnel XV-15 tests are also discussed.

As discussed earlier, a shaft angle (α_s) sweep was performed at an advance ratio (μ) of 0.125 (or M_{AT} = 0.69) at a blade loading coefficient (C_T/σ) of 0.075. The sweep was performed for shaft angles from -10 to 10° to identify a peak BVI flight condition. Figure 13 shows a) OASPL and b) BVISPL versus α_s for microphones 1 through 4 for this condition. The peak OASPL is at a shaft angle of 7° (Fig. 13 a) for all microphones, while the peak BVISPL is at a shaft angle of 0° (Fig. 13 b)).

The two peak shaft angle conditions are further investigated by comparing the unfiltered and filtered acoustic time history for microphone 1 (see Fig. 14). Figure 14 a) for a shaft angle of 0° shows a higher peak-to-peak BVI pulse compared to

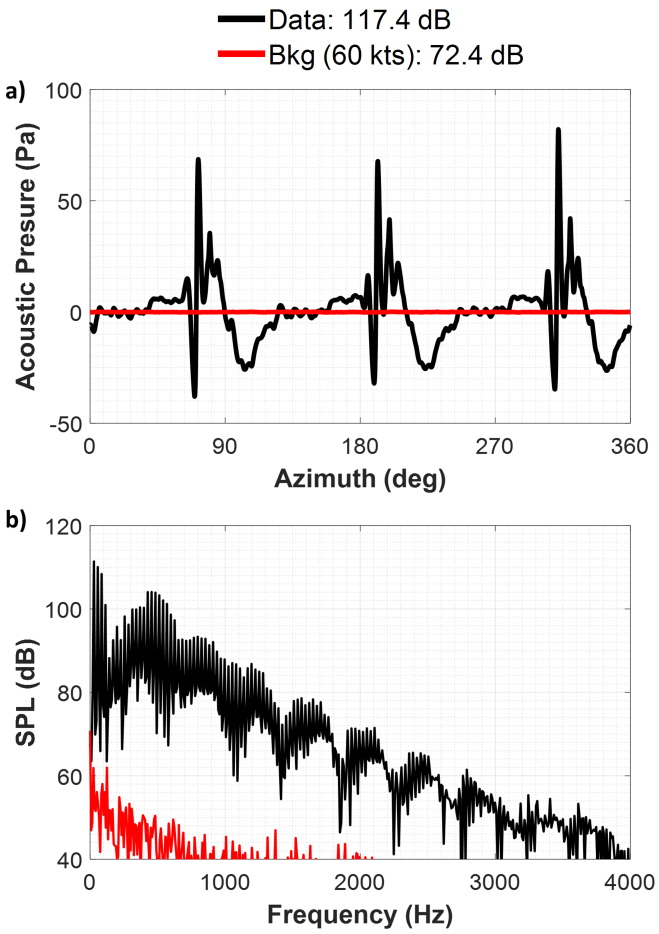

Fig. 9. a) Acoustic time history and b) frequency spectrum of TTR background noise (60 knots, α_s = 0°, blades off) and TTR at a flight conditions of μ = 0.125, M_{tip} = 0.684, C_T/σ = 0.075 and α_s = 0° in the NFAC 40- by 80-Foot Wind Tunnel.

7° (Fig. 14 b)). The BVI pulse is seen in the acoustic time history at an azimuth of 70, 190, and 310 degrees. OASPL is higher for a shaft angle of 7° due to a higher loading noise (low-frequency) component, seen in the acoustic time history at an azimuth of 105, 225, and 354 degrees. The first BVI and loading noise pulse component in the time history is identified in Fig. 14 a) with a blue dotted box at 70 and 105 degrees, respectively. Because BVI noise is investigated for this paper, the BVISPL will be used to compare data from this point on.

A thrust sweep was then performed at 0° shaft angle for a thrust of C_T/σ = 0.02 to 0.075 (see Fig. 15). For all microphones an overall positive slope in BVISPL for increasing thrust is shown, which indicates that BVI noise levels are sensitive to thrust for this specific flight condition.

Figure 16 shows BVISPL versus C_T/σ for α_s = -10, -5, 0, 5, and 10° for a flight condition of μ = 0.125 (M_{AT} = 0.77) for microphones a) 1 and b) 3. Figure 16 reveals that BVISPL is not directly proportional thrust or shaft angle for these conditions. In Fig. 15 for α_s = 0°, a global increase in BVISPL with increasing thrust was observed for all microphones, where

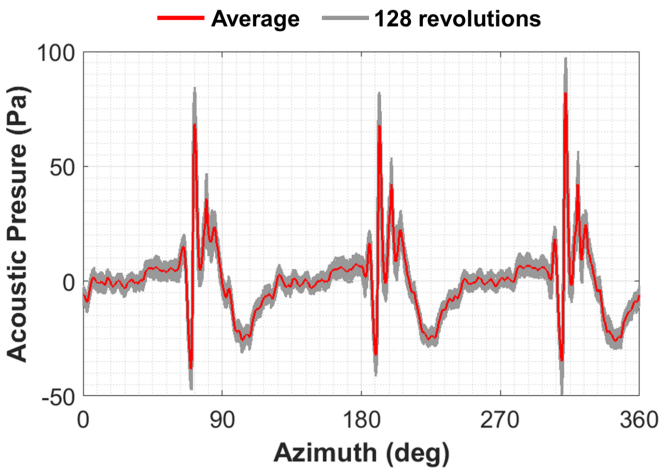

Fig. 10. TTR averaged (red) versus the 128 revolutions (gray) of a sample acoustic time history data for microphone 1 in the NFAC 40- by 80-Foot Wind Tunnel, for a flight condition of C_T/σ = 0.075, μ = 0.125, M_{tip} = 0.684, and α_s = 0°.

as with a different shaft angle the trend is different due to the behavior of the wake interacting with the rotor. Furthermore, due to the location of the microphones, the directivity of the source is different, resulting in different trends from microphone-to-microphone.

An example of the effects of advance ratio on BVI noise is shown in Fig. 17. Results are plotted in terms of advancing tip Mach number, however, remembering that $M_{AT} = (1+\mu)M_{tip}$. An advance ratio sweep was performed for α_s = -15° at C_T/σ = 0.100, see Fig. 17 a), where BVISPL generally increases for increasing advancing tip Mach number. An increasing BVISPL with advancing tip Mach number is also seen for the same shaft angle, but at C_T/σ = 0.050, in Fig. 17 b).

Comparison of TTR 699 and XV-15 rotor acoustic data

Acoustic time history data from the 1996 and 1999 NFAC 80- by 120-Foot Wind Tunnel XV-15 test were compared to the 2018 NFAC 40- by 80-Foot Wind Tunnel TTR test. While approximately of the same size and tested in similar operating conditions, there are differences in the geometry of the rotor and test condition that, although small, can potentially have an effect on the acoustic characteristics. The TTR rotor has a slightly longer chord and greater solidity. More importantly, rotors have different twist distributions, planform and airfoils, which can affect the loading distribution and geometry of the blade-vortex interaction. Different precone values could conceivably play a role influencing the blade-vortex separation. Although the non-dimensional parameters were approximately matched ($C_T/\sigma \approx 0.075$, $\mu \approx 0.12-0.13$, and $M_{tip} \approx 0.69$), it is therefore unrealistic to expect the rotors to exhibit identical peak BVI noise directivity characteristics.

Measurements from microphone 5 from 1996, and microphone 9 from 1999 in the NFAC 80- by 120-Foot Wind Tunnel

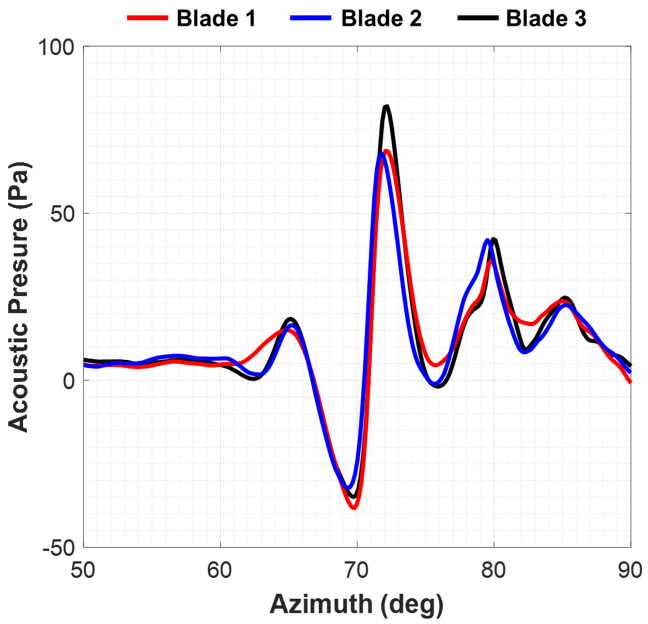

Fig. 11. Blade-to-blade comparison for TTR averaged acoustic time history data for microphone 1 in the NFAC 40- by 80-Foot Wind Tunnel, for a flight condition of C_T/σ = 0.075, μ = 0.125, M_{tip} = 0.684, and α_s = 0°.

are compared to microphone 3 from the NFAC 40- by 80-Foot Wind Tunnel in Figs. 18–20. The 2018 TTR acoustic data is corrected for distance accordingly by using the inverse-square law (Ref. 10).

For all three tests, similar flight conditions were chosen to perform an α_s sweep for $C_T/\sigma \approx 0.075$, $\mu \approx 0.12 - 0.13$, and $M_{tip} \approx 0.69$. Figure 18 shows BVISPL versus α_s for the three tests. The peak BVISPL for the 2018 TTR test occurred at α_s = 0°, while the nearest BVISPL peak for the 1996 and 1999 XV-15 occurred at $\alpha_s = 4°$.

The filtered time history for each test is analyzed to further investigate the difference. First, the peak BVISPL shaft angle (α_s = 0°) from the 2018 TTR test is compared to the same shaft angle from the 1996 and 1999 XV-15 test. Figure 19 shows a time history of a BVI pulse for the three microphones from the three different tests. The time history for the 2018 TTR test has a greater peak-to-peak value and pulse width compared to the 1996 and 1999 XV-15 data. The large difference between the three tests motivated the further analysis of this data set.

The peak BVISPL shaft angle from each test is then chosen and compared. Figure 20 shows microphone 3 from 2018 has a shaft angle of 0° and microphones 5 and 9 at a shaft angle of 4°. Compared to Fig. 19, Fig. 20 reveals an overall closer comparison between the three tests in terms of BVISPL, peak-to-peak, pulse width, and slope.

For the 2018 TTR test, initial estimates of angle of attack effects due to the presence of the wind tunnel walls (Glauert correction) suggests an additional positive angle of attack to be applied to the shaft angle (Refs. 11, 12). This may provide

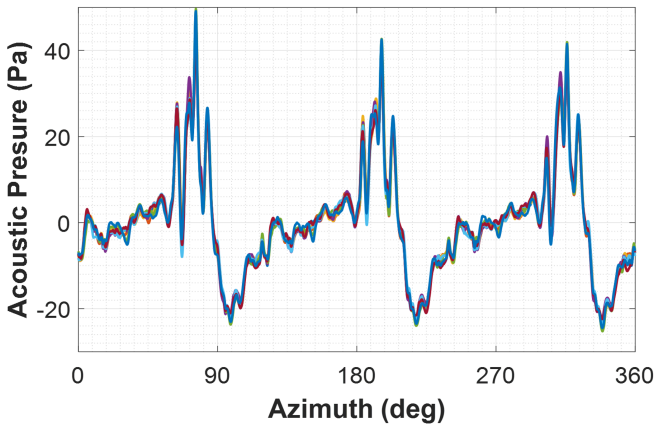

Fig. 12. TTR in the NFAC 40- by 80-Foot Wind Tunnel eight acoustic time histories from microphone 1 for a flight condition of μ = 0.125, M_{tip} = 0.684, C_T/σ = 0.050 and α_s = 0°. Time histories are from different runs on different days.

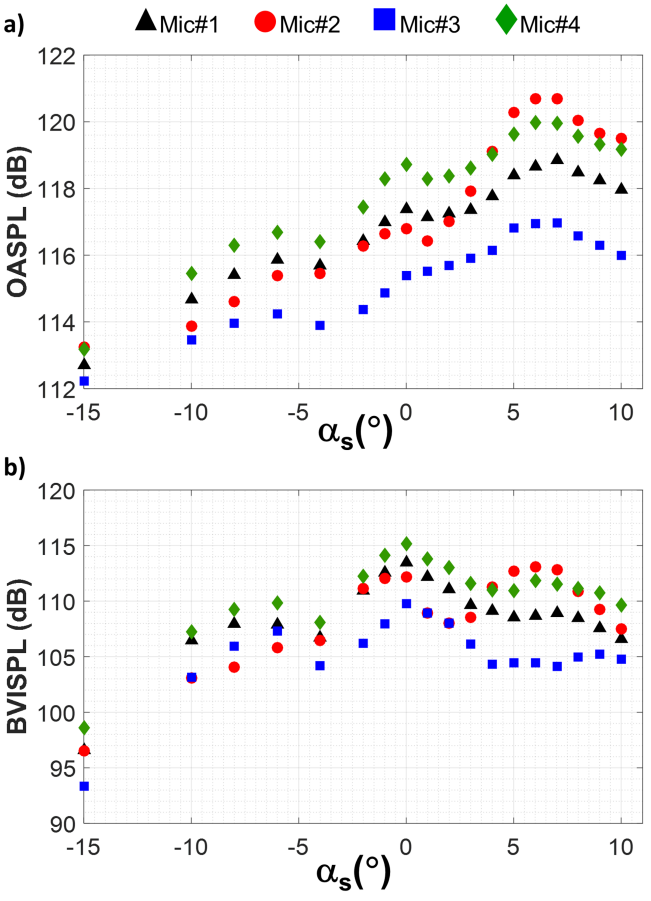

Fig. 13. TTR in the NFAC 40- by 80-Foot Wind Tunnel a) OASPL and b) BVISPL versus α_s for microphones 1 through 4 for a flight condition of C_T/σ = 0.075, μ = 0.125, and M_{tip} = 0.684.

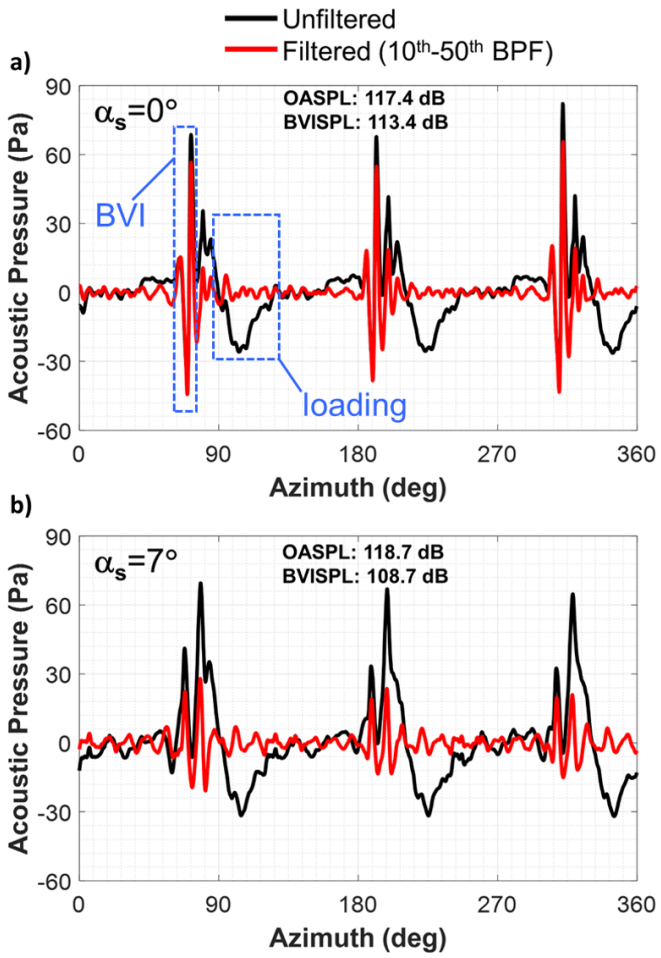

Fig. 14. TTR in the NFAC 40- by 80-Foot Wind Tunnel unfiltered and filtered acoustic time history for microphone 1 for a flight condition of C_T/σ = 0.075, μ = 0.125, M_{tip} = 0.684, at a) α_s = 0° and b) 7°.

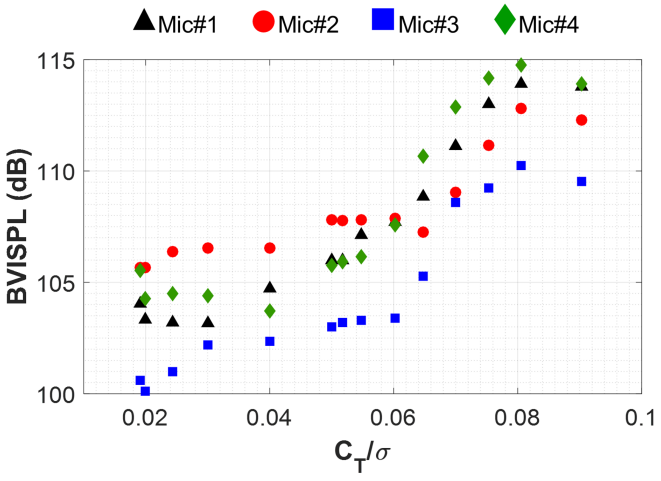

Fig. 15. TTR in the NFAC 40- by 80-Foot Wind Tunnel BVISPL versus C_T/σ for microphones 1 through 4 for a flight condition of μ = 0.125, M_{tip} = 0.684, and α_s = 0°.

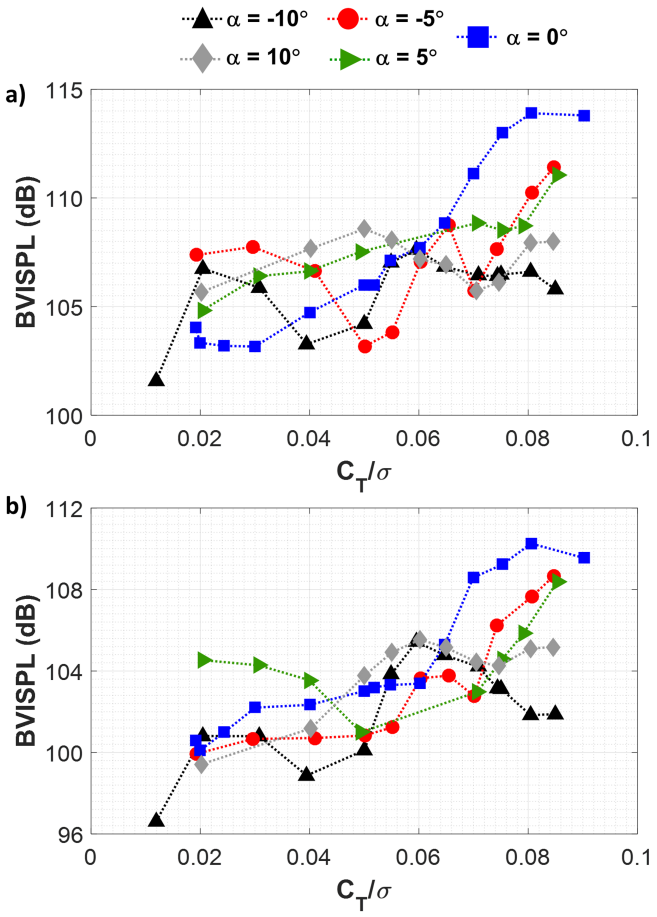

Fig. 16. TTR in the NFAC 40- by 80-Foot Wind Tunnel BVISPL versus C_T/σ for α_s = -10, -5, 0, 5, and 10° for a flight condition of μ = 0.125 (M_{AT} = 0.77) for microphone a) 1 and b) 3.

a partial explanation of the peak BVI shaft angle differences shown. At this time, however, differences in shaft angle due to wind tunnel wall effects have not been finalized.

CONCLUSIONS

The TTR check out was completed in the fall of 2018. Acoustic measurements were taken as part of the checkout. Four microphones were placed around the TTR to capture BVI and to match locations from previous tests in the NFAC 80- by 120-Foot Wind Tunnel for the XV-15 rotor. The following conclusions can be drawn from the acoustic data presented.

Existing concerns about the biases that may exist in the acquired acoustic measurements caused by reflections and standing waves at low frequencies and rotor proximity to the wind tunnel wall remain unaddressed. Further investigation and analysis is suggested.

A BVISPL metric was selected to match the previous tests in the NFAC 80- by 120-Foot Wind Tunnel for the XV-15 rotor and a quality assessment of the pulses confirmed that the bandpass filtering between the 10th and 50th accurately characterized the BVI noise.

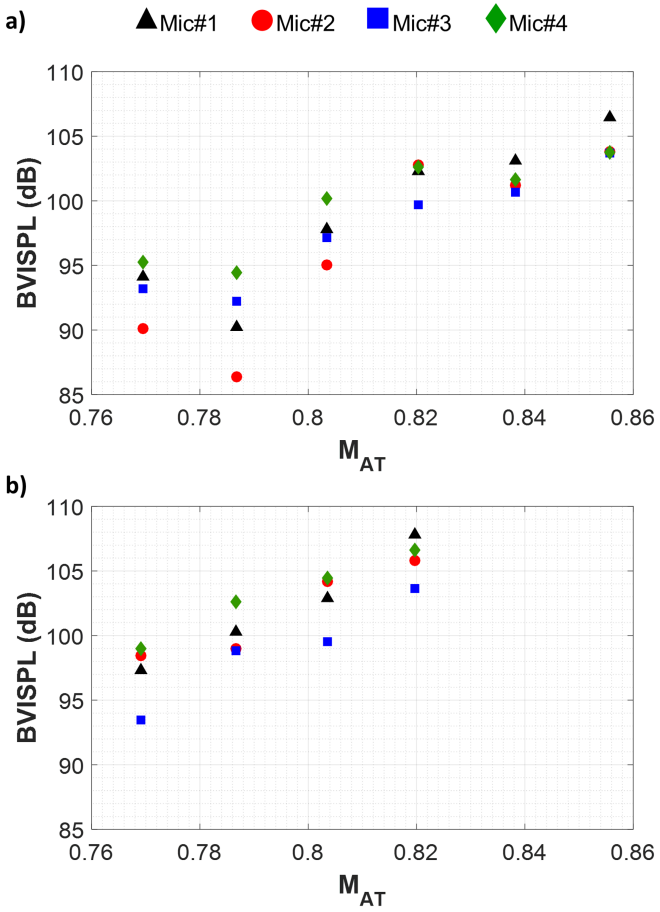

Fig. 17. TTR in the NFAC 40- by 80-Foot Wind Tunnel BVISPL versus M_{AT} for microphones 1 through 4 for a flight condition of α_s = -15° and at a) C_T/σ = 0.100, and b) C_T/σ = 0.050.

Aerotares were performed and revealed an adequate acoustic signal-to-noise ratio. In terms of background noise, minimal variance due to TTR shaft angle was shown in terms of OASPL and BVISPL.

Data repeatability was evaluated by comparing the rev-to-rev variability for a single data point, comparing the blade-to-blade variability for an averaged time history, and comparing average time histories for multiple data points. All three evaluations resulted in minimal variation, which suggests that the TTR setup in the NFAC 40- by 80-Foot Wind Tunnel is an adequate facility for acquiring acoustic data in terms of repeatability.

BVI trends were shown including a thrust, shaft angle and advance ratio sweep. The shaft angle sweep at $C_T/\sigma = 0.075$, μ = 0.125 and M_{tip} = 0.684 was shown and compared to data from the XV-15 tests from 1996 and 1999. For the 2018 TTR test, a peak BVI shaft angle was identified at 0°, which differed from the previous XV-15 rotor tests. Differences in acoustic characteristics between the tests are likely due to the variation in blade geometry and the proximity of the rotor to the wind tunnel wall.

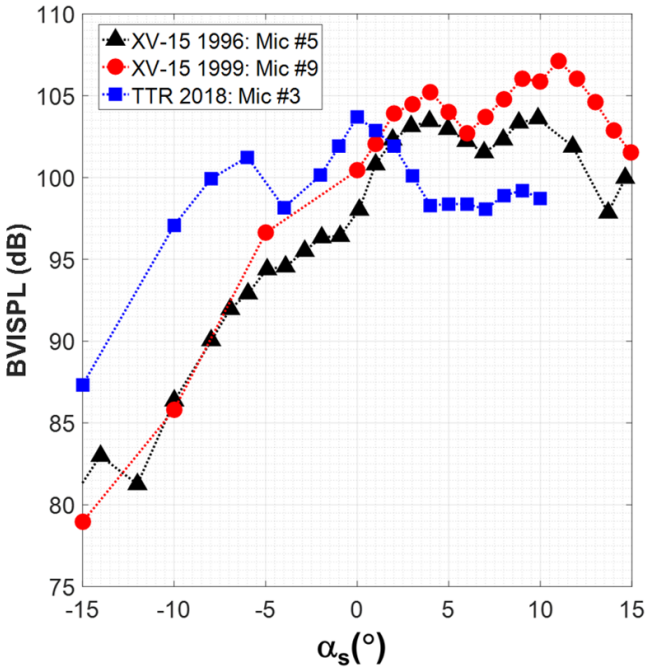

Fig. 18. BVISPL versus α_s for microphones 5 and 9 from 1996 and 1999 in NFAC 80- by 120-Foot Wind Tunnel of the XV-15 test and microphone 3 from the 2018 NFAC 40- by 80-Foot Wind Tunnel TTR test at $C_T/\sigma \approx 0.075$, $\mu \approx 0.12-0.13$, and $M_{tip} \approx 0.69$.

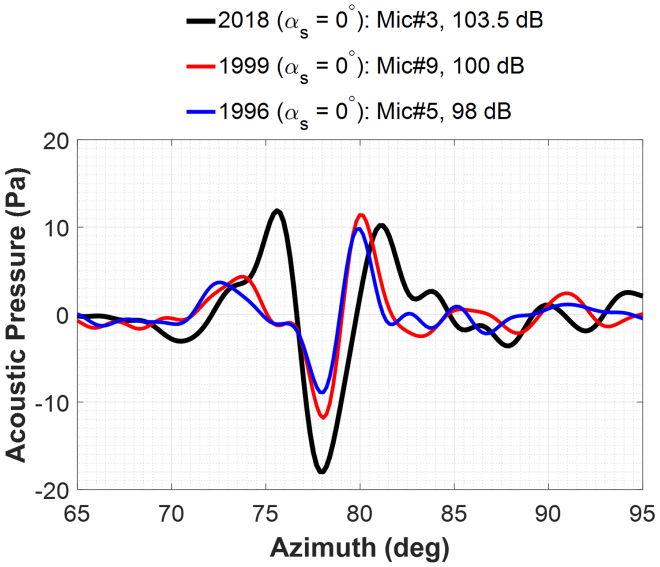

Fig. 19. Acoustic time history of microphones 5 and 9 from 1996 and 1999 in NFAC 80- by 120-Foot Wind Tunnel of the XV-15 test and microphone 3 from the 2018 NFAC 40- by 80-Foot Wind Tunnel TTR test at α_s = 0°, $C_T/\sigma \approx 0.075$, $\mu \approx 0.12-0.13$, and $M_{tip} \approx 0.69$

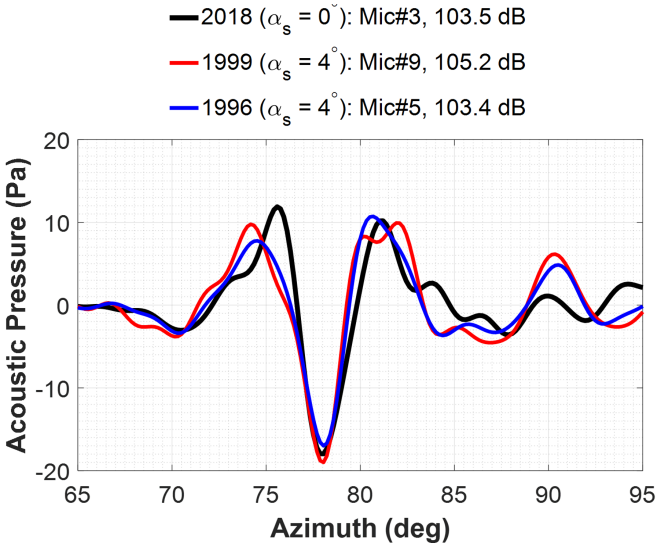

Fig. 20. Acoustic time history of microphones 5 and 9 from 1996 and 1999 in NFAC 80- by 120-Foot Wind Tunnel of the XV-15 test at α_s = 4° and microphone 3 from the 2018 NFAC 40- by 80-Foot Wind Tunnel TTR test at α_s = 0° ($C_T/\sigma \approx 0.075$, $\mu \approx 0.12 - 0.13$, and $M_{tip} \approx 0.69$).

ACKNOWLEDGMENTS

This paper is dedicated to Dr. Ben Wel-C. Sim.

Dr. Sim participated in the acoustic set up and recording of the acoustic data in the NFAC 40- by 80-Foot Wind Tunnel. We thank him for his professional guidance and friendship. We are honored to have had the opportunity to learn from him. Thank you Ben.

REFERENCES

[1]Acree, C. W., Jr., and Sheikman, A. L., "Development and Initial Testing of the Tiltrotor Test Rig," American Helicopter Society 74th Annual Forum, Phoenix, AZ, May 14-17, 2018.

[2]Kottapalli, S. and Acree, C. W., "Correlation of Full-Scale Isolated Proprotor Performance and Loads," Vertical Flight Society 75th Annual Forum, Philadelphia, PA, May 2019.

[3]Acree, C. W., Sheikman, A. L., and Norman, T. R., "High-Speed Wind Tunnel Tests of a Full-Scale Proprotor on the Tiltrotor Test Rig," Vertical Flight Society 75th Annual Forum, Philadelphia, PA, May 2019.

[4]Kitaplioglu, C., "Blade–Vortex Interaction Noise of a Full-Scale XV-15 Rotor Tested in the NASA Ames 80-by 120-Foot Wind Tunnel," NASA TM 1999-208789, July 1999.

[5]Kitaplioglu, C., McCluer, M., and Acree, Jr., C. W., "Comparison of XV-15 Full-Scale Wind Tunnel and In-Flight Blade-Vortex Interaction Noise," American Helicopter Society 53rd Annual Forum, Virginia Beach, VA, April 1997.

[6]Kitaplioglu, C and Betzina, M and Johnson, W., "Blade-Vortex Interaction Noise of an Isolated Full-Scale XV-15 Tilt-Rotor," American Helicopter Society 56th Annual Forum, Virginia Beach, VA, May 2-4, 2000.

[7]Barbely, N., Kitaplioglu, C., and Sim, W., "Acoustics Reflections of Full-Scale Rotor Noise Measurements in NFAC 40-by 80-Foot Wind Tunnel," American Helicopter Society Specialists' Conference, San Francisco, CA, January 20-21, 2012.

[8]Narramore, J.C., "Airfoil Design, Test, and Evaluation for the V-22 Tilt Rotor Vehicle," American Helicopter Society 43rd Annual Forum, St. Louis, MO, May 18-24, 1987.

[9]Narramore, J. C., Platz, D. A., and Brand, A. G., "Application of Computational Fluid Dynamics to the Design of the BA 609," 25th European Rotorcraft Forum, Rome, Italy, September 1999.

[10]Kinsler, L.E., Frey, A.R., Coppens, A.B. and Sanders, J.V., " Fundamentals of Acoustics," 4th Edition. ISBN 0-471-84789-5. Wiley-VCH, December 1999.

[11]Langer, H., Peterson, L., and Maier,T., "An experimental evaluation of wind tunnel wall correction methods for helicopter performance," American Helicopter Society 52nd Annual Forum, Washington, D.C., June 4-6, 1996.

[12]Glauert, H., "The Interference on the Characteristics of an Airfoil in a Wind Tunnel of Rectangular Section," R & M 1459, 1932.

[13]Koushik, S., and Schmitz, F.H., "Understanding In-Plane Helicopter Blade-Vortex Interaction (BVI) Noise," American Helicopter Society 68th Annual Forum, Fort Worth, TX, May 1-3, 2012.